Quantum black holes: Nonperturbative corrections and no-veil scenario

Jorge G. Russo
Theory Group, Department of Physics, University of Texas, Austin, Texas 78712
(Received 2 August 1993)

A common belief is that further quantum corrections near the singularity of a large black hole should not substantially modify the semiclassical picture of black hole evaporation; in particular, the outgoing spectrum of radiation should be very close to the thermal spectrum predicted by Hawking. In this paper we explore a possible counterexample: in the context of dilaton gravity, we find that nonperturbative quantum corrections which are important in strong-coupling regions may completely alter the semiclassical picture, to the extent that the presumptive spacelike boundary becomes timelike, changing in this way the causal structure of the semiclassical geometry. As a result, only a small fraction of the total energy is radiated outside the fake event horizon; most of the energy comes in fact at later retarded times and there is no problem of information loss. This may constitute a general characteristic of quantum black holes, that is, quantum gravity might be such as to prevent the formation of global event horizons.

PACS number(s): 04.70.Dy, 04.60.Kz

I. INTRODUCTION

The proposal by Hawking that black holes evaporate by emitting thermal radiation [1] led to a puzzling and confusing status about the fate of quantum information in gravitational collapse. In particular, this proposal entails allowing pure states to evolve into mixed states, requiring a modified version of quantum mechanics in order to accommodate loss of quantum coherence [1]. This proposal was received with some criticism by different authors [see e.g., Ref. [2]), but so far an understanding of the phenomenon has not been achieved. Apart from the existence of a mathematical framework which may reconcile Hawking's observation with quantum mechanics, information loss raises a serious question of principle for observers who do not fall into black holes, their future being uncorrelated to their past. Several attempts have been made to provide alternative ways before accepting that quantum-mechanical information is simply lost in the process of black hole evaporation. Thus far the proposals fall into either one of the two following categories: (1) by the end of the evaporation process there is a Planckian-size stable or long-lived remnant that still contains the information; (2) the back reaction to the emission of radiation and quantum corrections introduce subtle correlations between different modes, allowing the information to come out continuously encoded in the Hawking radiation, the process being described by a unitary S matrix. These two approaches are not exempt from criticism. The first has problems with *CPT* and also with thermodynamics. The second possibility seems to imply acausal propagation of the information, since this was carried far beyond the horizon before the curvature is strong enough for quantum gravitational effects to be important. To avoid the serious problem of acausality, a rather temerarious proposal that has recently been revived [3-5] consists in postulating that the information is duplicated at the moment it crosses the horizon. This interpretation requires Planckian physics occurring in the vicinity of the horizon, and implies a dual description of reality at macroscopic levels.

In this paper we explore a more conservative possibility which does not belong to the schemes (1) and (2) mentioned above. Figure 1(a) is a Penrose diagram representing the standard picture of semiclassical black hole evaporation, which is reliable in the region away from the singularity. Figure 1(b) completely agrees with Fig. 1(a) in all regions where the semiclassical equations of motion are supposed to apply, but instead of a singularity there is simply a strong curvature region, and the actual boundary of the space time is timelike. This requires boundary conditions. Let us assume that some sort of reflecting boundary conditions can be imposed there and may lead to a finite curvature on the boundary, just as it happens in the low-energy sector of the two-dimensional model of Refs. [6,7], which we shall review in Sec. II. The causal structure of Fig. 1(b) is completely different from the causal structure of Fig. 1(a), and therefore one would expect that the corresponding spectra of outgoing Hawking radiation should be distinct, perhaps in a crucial way. In fact, this turns out to be the case. Given a geometry like Fig. 1(b), with reflecting-type boundary conditions on the timelike boundary, most of the energy will appear in the region in causal contact with the timelike boundary, i.e., far beyond the fake event horizon, and thus there is no information loss problem. The resulting picture is in some sense similar to the low-energy sector of Refs. [6,7], and it does not differ much from an accelerating mirror. The boundary of space time actually being timelike, there is no longer any reason to believe that a unitary S matrix for the model cannot be constructed. Another similar scenario will be mentioned in Sec. VI.

II. SEMICLASSICAL DILATON GRAVITY

A simplified model for black hole formation and evaporation, known as the CGHS model, was introduced in Ref. [8]. This model permits one to study the Hawking

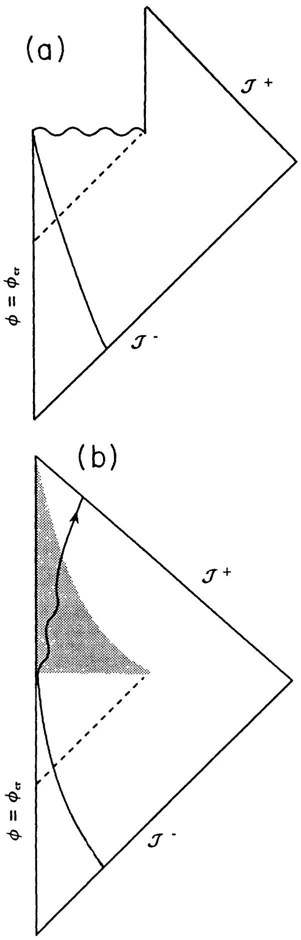

FIG. 1. (a) Penrose diagram corresponding to the standard semiclassical picture of black hole evaporation. (b) Penrose diagram of another geometry which differs from Fig. 2(a) only in the strong curvature region. In the scenario there is no spacelike boundary.

phenomenon in detail, avoiding all the mathematical complications of higher-dimensional theories. Different discussions on two-dimensional dilaton gravity can be found, e.g., in Refs. [6–25]. Let us consider the model introduced in Ref. [6]. In the conformal gauge $g_{++}=g_{--}=0$, $g_{+-}=-\frac{1}{2}e^{2\rho}$, the effective action containing the conformal anomaly can be written as

$$S=\frac{1}{\pi}\int d^2x\left[-\partial_+\chi\partial_-\chi+\partial_+\Omega\partial_-\Omega+\lambda^2 e^{(2/\sqrt{\kappa})(\chi-\Omega)}+\frac{1}{2}\sum_{i=1}^{N}\partial_+f_i\partial_-f_i\right], \tag{2.1}$$

where f_i are N-conformal fields, $\kappa=(N-24)/12>0$, and

$$\Omega=\frac{\sqrt{\kappa}}{2}\phi+\frac{e^{-2\phi}}{\sqrt{\kappa}}\ ,\quad \chi-\Omega=\sqrt{\kappa}(\rho-\phi)\ . \tag{2.2}$$

The constraints are

$$\kappa t_\pm(x^\pm)=-\partial_\pm\chi\partial_\pm\chi+\partial_\pm\Omega\partial_\pm\Omega+\sqrt{\kappa}\partial_\pm^2\chi+\frac{1}{2}\sum_{i=1}^{N}\partial_\pm f_i\partial_\pm f_i\ . \tag{2.3}$$

The functions $t_\pm(x^\pm)$ reflect the nonlocal nature of the anomaly and are determined by boundary conditions. The solution to the semiclassical equations of motion and the constraints, for general distributions of incoming matter, is given in Kruskal coordinates by

$$\Omega=\chi=-\frac{\lambda^2}{\sqrt{\kappa}}x^+\left[x^-+\frac{1}{\lambda^2}P_+(x^+)\right]+\frac{M(x^+)}{\sqrt{\kappa}\lambda}-\frac{\sqrt{\kappa}}{4}\ln(-\lambda^2x^+x^-)\ , \tag{2.4}$$

where $M(x^+)$ and $P_+(x^+)$, respectively, represent total energy and Kruskal momentum of the incoming matter at advanced time x^+:

$$M(x^+)=\lambda\int_0^{x^+}dx^+x^+T_{++}(x^+)\ ,$$
$$P_+(x^+)=\int_0^{x^+}dx^+T_{++}(x^+)\ . \tag{2.5}$$

In the case $T_{++}=0$ one obtains the familiar linear dilaton vacuum, $e^{-2\phi}=e^{-2\rho}=-\lambda^2x^+x^-$.

Generically, there will be a curvature singularity at $\phi=\phi_{\rm cr}=-\frac{1}{2}\ln(\kappa/4)$, which can be regarded as the boundary of the space time.

Let us assume that originally the geometry is the linear dilaton vacuum and at some time, which we arbitrarily set at $x^+=1/\lambda$, the incoming flux is turned on. As observed in Ref. [6], there are two different regimes, according to whether the incoming matter energy-momentum tensor is less or greater than a critical flux

$$T_{++}^{\rm cr}(x^+)=\frac{\kappa}{4}\frac{1}{x^{+2}}\ . \tag{2.6}$$

In the supercritical regime the line $\phi=\phi_{\rm cr}$ is spacelike and one has a time-dependent geometry representing the process of formation and evaporation of a black hole (see Fig. 2). At the end-point line, $x^-=x_s^-$, $x^+>x_s^+$, it is possible to match the solution continuously with the linear dilaton vacuum.

In the subcritical regime the boundary is timelike and one needs boundary conditions in order to determine the evolution in the region in causal contact with the timelike boundary (see Fig. 3). It turns out that there are natural, reflecting-type boundary conditions which uniquely determine the evolution and implement the cosmic censorship hypothesis [7]; they are in fact the only possible boundary conditions which lead to a finite curvature on the boundary line.

The curvature scalar is $R=8e^{-2\rho}\partial_+\partial_-\rho$, where

$$\partial_+\partial_-\rho=\frac{1}{\Omega'}\left[\partial_+\partial_-\chi-\frac{4e^{-2\phi}}{\sqrt{\kappa}}\partial_+\phi\partial_-\phi\right]\ . \tag{2.7}$$

At $\phi=\phi_{\rm cr}$ one has $\Omega'(\phi)=0$. In the Kruskal gauge, $\partial_+\partial_-\chi=-\lambda^2/\sqrt{\kappa}$. Therefore, in order for the curvature to be finite at $\phi=\phi_{\rm cr}$, it is necessary that

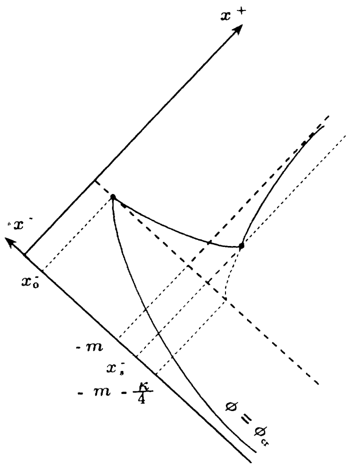

FIG. 2. Standard semiclassical picture of black hole evaporation in Kruskal coordinates, corresponding to gravitational collapse of an incoming shock wave ($\lambda=1$).

$$\partial_+\phi\partial_-\phi=-\frac{\lambda^2}{\kappa}\ .$$

In particular, this implies [cf. Eq. (2.2)]

$$\partial_+\Omega|_{\phi=\phi_{cr}}=\partial_-\Omega|_{\phi=\phi_{cr}}=0\ . \tag{2.8}$$

As a result, the solution in region (ii) is given by

$$\Omega^{(ii)}(x^+,x^-)=\Omega^{(i)}(x^+,x^-)+F(x^-)\ , \tag{2.9}$$

where $\Omega^{(i)}$ is given by Eq. (2.4),

$$F(x^-)=\frac{\sqrt{\kappa}}{4}\ln(-\lambda^2x^-\hat{x}^+)-\frac{M(\hat{x}^+)}{\sqrt{\kappa}\lambda}-\frac{\sqrt{\kappa}}{4}\ln\left[\frac{\kappa}{4}\right]\ , \tag{2.10}$$

and $\hat{x}^+(x^-)$ is the boundary curve given by

$$\frac{\kappa}{4}=-\lambda^2\hat{x}^+\left[x^-+\frac{1}{\lambda^2}P_+(\hat{x}^+)\right]\ . \tag{2.11}$$

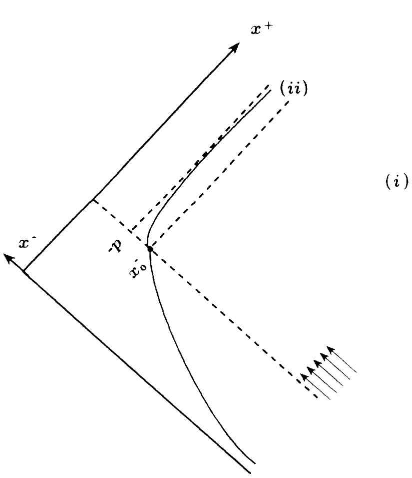

FIG. 3. A subcritical incoming energy flux leads to a timelike singularity.

In Ref. [7] it was shown that these boundary conditions conserve energy. Let $m\equiv M(\infty)$ and $p\equiv P_+(\infty)$. The outgoing energy fluxes $T_{--}(x^-)$ regions (i) and (ii) are, respectively,

$$T_{--}^{(i)}(x^-)=\frac{\kappa}{4}\left[\frac{1}{[x^-+(1/\lambda^2)p]^2}-\frac{1}{x^{-2}}\right]\ , \tag{2.12}$$

$$T_{--}^{(ii)}(x^-)=\frac{\kappa}{4}\frac{1}{[x^-+(1/\lambda^2)p]^2}-\frac{\lambda^4}{\kappa/4\hat{x}^+-\hat{x}T_{++}(\hat{x}^+)}\ . \tag{2.13}$$

Note that $T_{--}^{(i)}(x^-)\sim 0$ for $x^-\ll x_1^-=-p/\lambda^2$.

The total radiated energies in regions (i) and (ii) are

$$\begin{aligned}E_{\rm out}^{(i)}&=-\lambda\int_{-\infty}^{x_0^-}dx^-\left[x^-+\frac{1}{\lambda^2}p\right]T_{--}^{(i)}\\&=p-\frac{\kappa\lambda}{4}\ln\left[1-\frac{4p}{\kappa\lambda}\right]\ ,\end{aligned} \tag{2.14}$$

$$\begin{aligned}E_{\rm out}^{(ii)}&=-\lambda\int_{x_0^-}^{x_1^-}dx^-\left[x^-+\frac{1}{\lambda^2}p\right]T_{--}^{(ii)}\\&=m-p+\frac{\kappa\lambda}{4}\ln\left[1-\frac{4p}{\kappa\lambda}\right]\ .\end{aligned} \tag{2.15}$$

A close examination of Eqs. (2.12)–(2.15) shows that for low-energy fluxes one has

$$E_{\rm out}^{(i)}\ll m\ ,\quad E_{\rm out}^{(ii)}\sim m\ , \tag{2.16}$$

that is, most of the energy comes out by pure reflection on the space-time boundary.

Instead, for energy fluxes near the critical value, one may have $E_{\rm out}^{(i)}>m$ and $E_{\rm out}^{(ii)}<0$. This implies that the semiclassical approximation is breaking down some Planck units before entering into region (ii). Perhaps nonperturbative contributions are already important.

III. NONPERTURBATIVE QUANTUM CORRECTIONS

The form of the quantum effective action which includes the quantum anomaly term of exact semiclassical dilaton gravity [9,14,15,16] follows by a DDK-type argument [26]. Instead of using an invariant regularization (which is complicated in the conformal gauge) one adopts a noninvariant cutoff adding at the same time some counterterms which are necessary in order to satisfy the reparametrization invariant Ward identities. The resulting "effective action" should generate a theory which is invariant under the background Weyl symmetry, $\hat{g}\to e^{2\tau(x)}\hat{g}$, $\rho(x)\to\rho(x)-\tau(x)$, where $\hat{g}$ is a background metric. Since the metric $g=e^{2\rho}\hat{g}$ is left unchanged, this transformation should be an exact symmetry of the theory, i.e., the β functions of the couplings in the "effective action" should vanish. The basic assumption is that the conformal factor dependence of the covariant quantum measure and regularization can be represented by a local effective action containing only the simplest, lowest derivative terms. The kinetic term of the resulting quantum effective action is modified by the Weyl anomaly term and also by possible counterterms, and one automatically attains a partial resummation of the standard loop expansion. In particular, this procedure also generates counterterms which are of nonperturbative nature, e.g., of the form $e^{-1/g^2}=\exp(-e^{-2\phi})$.

Thus one considers the two-dimensional σ model with fields ρ and ϕ and fixes the couplings by demanding conformal invariance. Since the target metric is flat, it is possible to go to the diagonal parametrization χ and Ω which simplifies the equations of motion, as found in Ref. [14]. To leading order, the β function corresponding to the "tachyonic" coupling is given by

$$\beta^V=\left[\frac{\partial^2}{\partial\chi^2}-\frac{\partial^2}{\partial\Omega^2}+\frac{1}{2}\sqrt{\kappa}\frac{\partial}{\partial\chi}-1\right]V(\chi,\Omega)\ . \quad (3.1)$$

The potential $\lambda^2 e^{(2/\sqrt{\kappa})(\chi-\Omega)}$ employed in Sec. II [see Eq. (2.1)] is, in fact, a particular solution to this equation. The most general solution is

$$V(\chi,\Omega)=\int da[v^+(a)e^{a\chi+b\Omega}+v^-(a)e^{a\chi-b\Omega}]\ , \quad (3.2)$$

with

$$b=-\sqrt{a^2+\sqrt{\kappa}/2a-1}\ . \quad (3.3)$$

However, we are interested in solutions which in the weak coupling region $e^{\phi}\to 0$ lead to the classical CGHS action. From Eq. (2.2) we deduce that this requires the condition

$$a+b\le 0\ .$$

Thus the general potential which leads to the CGHS action in the weak-coupling regime is

$$V(\chi,\Omega)=\lambda^2 e^{(2/\sqrt{\kappa})(\chi-\Omega)}+\int_{2/\sqrt{\kappa}}^{\infty}da\ v(a)e^{a\chi+b\Omega}\ . \quad (3.4)$$

The second term will contain nonperturbative contributions of the form $\exp([(a+b)/\sqrt{\kappa}]e^{-2\phi})$. At full quantum level one expects that all physical quantities should be plagued by nonperturbative corrections, originating from strong curvature regions.

The semiclassical equations of motion become complicated when the general potential (3.4) is adopted. In order to elucidate the basic idea, let us consider a simple model with the action given by

$$S=\frac{1}{\pi}\int d^2x\left[-\partial_+\chi\partial_-\chi+\partial_+\Omega\partial_-\Omega+\lambda^2 e^{(2/\sqrt{\kappa})(\chi-\Omega)}+\mu e^{a\chi+b\Omega}+\frac{1}{2}\sum_{i=1}^{N}\partial_+f_i\partial_-f_i\right]\ , \quad (3.5)$$

where Ω and χ are given in terms of ϕ and ρ as in Eq. (2.2), μ is for the moment arbitrary, $a>2/\sqrt{\kappa}$, and b is given by Eq. (3.3). The RST model is a particular case with $\mu=0$.

In principle, nonperturbative corrections may be different for distinct geometries. In particular, it may be that the linear dilaton vacuum does not receive any correction at all, the curvature being zero everywhere. Unfortunately, a systematic derivation of the DDK ansatz, i.e., calculating loops with covariant regularization, etc., is lacking, so it is unclear what should be the value of μ in the "phenomenological" action (3.5). The only independent constants of the theory are λ and κ. Therefore μ should be given in terms of λ, κ, and maybe other parameters characterizing the geometry, the ADM mass, *verbigratia,* or the moments

$$P_+^n=\int_0^{\infty}dx^+(x^+)^{-n+1}T_{++}(x^+)\ ,\quad n\in\mathbb{N}\ . \quad (3.6)$$

In the particular case of a shock-wave geometry, which will be investigated in detail below, μ would only depend on λ, κ, and the total ADM energy carried by the collapsing matter. The essential point, i.e., that nonperturbative corrections can change the space-time topology by turning the boundary curve from spacelike to timelike, is a quite generic result, holding true for a wide range of choices for μ.

Models with different potentials which represent an Einstein-Maxwell system have been extensively studied in Refs. [17–19]. In those models there is also a regime where the singularity is timelike, as is the case for the Reissner-Nordström black hole. These models typically have a global horizon. In the present example μ will not be regarded as an arbitrary parameter of the potential, but depending on the ADM mass [see, e.g., Eqs. (5.1), (5.2)]. In particular, there will be, at most, a small Planck-order correction for the linear dilaton vacuum, as one would expect. The scope of this section is to prove that the natural nonperturbative terms appearing in Eq. (3.4), which are only important in strong curvature regions, can modify the causal structure of the geometry. In Sec. V we will illustrate the scenario by a numerical study of a particular model.

The equations of motion are

$$\partial_+\partial_-X=Ae^Y\ , \quad (3.7)$$

$$\partial_+\partial_-Y=Be^X+Ce^Y\ , \quad (3.8)$$

where

$$X=\frac{2}{\sqrt{\kappa}}(\chi-\Omega)\ ,\quad Y=a\chi+b\Omega\ , \quad (3.9)$$

and

$$A=-\frac{\mu}{\sqrt{\kappa}}(a+b)\ ,\quad B=-\frac{\lambda^2}{\sqrt{\kappa}}(a+b)\ ,$$

$$C=\frac{\mu}{2}(b^2-a^2)\ . \quad (3.10)$$

A particular solution $X=Y+\text{const.}$ is easily found, for which the system reduces to the Liouville equation. Unfortunately, this solution does not satisfy the asymptotic conditions corresponding to black hole configurations, and thus it is uninteresting for our purposes.

Although the general solution to the above system of nonlinear, partial differential equations has not been written in closed form, to our knowledge, it is nevertheless possible to obtain some exact, interesting results, as we shall see below.

To leading order in an expansion in powers of

$$\varepsilon=\exp\left[\frac{(a+b)}{\sqrt{\kappa}}e^{-2\phi}\right],$$

the general solution can be explicitly found by direct integration. Let us consider the case of a shock-wave geometry representing an infalling shell of matter by patching together a vacuum configuration on the inside and, on the outside, a solution which asymptotically corresponds to a black hole. Let us write

$$X=X_{sc}+O(\varepsilon)\ ,\quad Y=Y_{sc}+O(\varepsilon)\ . \tag{3.11}$$

where, in Kruskal coordinates,

$$X_{sc}=0\ , \tag{3.12}$$

$$Y_{sc}=(a+b)\left[\frac{m}{\lambda\sqrt{\kappa}}-\frac{\lambda^2}{\sqrt{\kappa}}x^+\left(x^-+\frac{m}{\lambda^2}\right)\right]-(a+b)\frac{\sqrt{\kappa}}{4}\ln(-\lambda^2x^+x^-)\ ,\quad x^+\geq 1/\lambda\ . \tag{3.13}$$

Now let us pick some convenient value for a which will simplify the calculation. For $\kappa>16$ we can choose $a+b=-4\sqrt{\kappa}$, i.e.,

$$a=\frac{2}{\sqrt{\kappa}}\frac{\kappa+16}{\kappa-16}\ . \tag{3.14}$$

For this value of a we have

$$e^{Y_{sc}}=-\lambda^2x^+x^-\exp\left[\frac{4\lambda^2}{\kappa}x^+\left(x^-+\frac{m}{\lambda^2}\right)-\frac{4m}{\kappa\lambda}\right] \tag{3.15}$$

and

$$A=\frac{4\mu}{\kappa}\ ,\quad B=\frac{4\lambda^2}{\kappa}\ ,\quad C=\frac{16\mu}{\kappa-16}\ . \tag{3.16}$$

The equations of motion take the form

$$\partial_+\partial_-X=Ae^{Y_{sc}}+O(\varepsilon^2)\ , \tag{3.17}$$

$$\partial_+\partial_-Y=B(1+X)+Ce^{Y_{sc}}+O(\varepsilon^2)\ . \tag{3.18}$$

These equations can now be solved by direct integration. The solution is so uniquely determined by the boundary conditions that at $x^-\ll 0$ it must approach the semiclassical solution, Eqs. (3.12), (3.13), and, on the infalling line $x^+=1/\lambda$, it must reduce to the linear dilaton vacuum. We find

$$X=\frac{\mu\kappa}{4\lambda^2}\left\{e^{-4m/\lambda\kappa}\mathrm{Ei}(-r)-e^{-4m/\lambda\kappa}\mathrm{Ei}\left[\frac{4\lambda}{\kappa}\left(x^-+\frac{m}{\lambda^2}\right)\right]-\frac{x^-}{x^-+m/\lambda^2}\left(e^{-4m/\lambda\kappa}e^{-r}-e^{(4\lambda/\kappa)x^-}\right)\right\}, \tag{3.19}$$

$$Y=-r-\frac{4m}{\kappa\lambda}+\ln(-\lambda^2x^+x^-)+y(x^+,x^-)-y\left(\frac{1}{\lambda},x^-\right), \tag{3.20}$$

where

$$y(x^+,x^-)=\mu e^{-4m/\lambda\kappa}x^+\left(x^-+\frac{2m}{\lambda^2}\right)\left\{\mathrm{Ei}(-r)-\mathrm{Ei}\left[\frac{4\lambda}{\kappa}\left(x^-+\frac{m}{\lambda^2}\right)\right]\right\}-\frac{\kappa\mu}{4\lambda^2}e^{-4m/\lambda\kappa}\left[2\mathrm{Ei}(-r)+\frac{\lambda^2x^-+2m}{\lambda^2x^-+m}e^{-r}\right]$$
$$+\frac{\kappa^2\mu}{(\kappa-16)\lambda^2}e^{-4m/\lambda\kappa}\left[\mathrm{Ei}(-r)-\frac{x^-}{x^-+m/\lambda^2}e^{-r}\right]+\frac{\kappa\mu}{2\lambda}x^+e^{(4\lambda/\kappa)x^-}\ , \tag{3.21}$$

$$r\equiv-\frac{4\lambda^2}{\kappa}x^+\left(x^-+\frac{m}{\lambda^2}\right),\quad \mathrm{Ei}(-r)=\int_\infty^r du\frac{e^{-u}}{u}\ . \tag{3.22}$$

Let us first consider $\kappa\sim 16$. In this case some terms can be ignored, which renders the analysis simpler. We obtain

$$\chi=\Omega=-\frac{\lambda^2}{4}x^+\left(x^-+\frac{m}{\lambda^2}\right)+\frac{m}{4\lambda}-\ln(-\lambda^2x^+x^-)+\frac{128\mu}{\lambda^2(\kappa-16)}$$
$$\times\left\{\frac{x^-}{x^-+\frac{m}{\lambda^2}}\left(e^{-m/4\lambda}e^{-r}-e^{(\lambda/4)x^-}\right)-e^{-m/4\lambda}\mathrm{Ei}(-r)+e^{-m/4\lambda}\mathrm{Ei}\left[\frac{1}{4}\left(x^-+\frac{m}{\lambda^2}\right)\right]\right\}. \tag{3.23}$$

The points where $\partial_+\Omega=0$ indicate the position of the apparent horizon (for a review of apparent horizon in $1+1$ dimensions, see Appendix). The apparent horizon of the border where the curves of constant ϕ change from timelike to spacelike and conversely. From Eq. (3.23) one obtains

$$\partial_+\Omega=-\frac{\lambda^2}{4}\left[x^-+\frac{m}{\lambda^2}\right]-\frac{1}{x^+}+\frac{32\mu}{\kappa-16}e^{-m/4\lambda}e^{-r}\left[x^--\frac{4}{\lambda^2x^+}\right]. \quad (3.24)$$

The line $\phi=\phi_{cr}$ intersects $x^+=1/\lambda$ at $x_0^-=-\kappa/4\lambda$. An inspection of Eq. (3.24) reveals that the equation $\partial_+\Omega=0$ may admit more than one solution in the physical region $x^-<x_0^-$ of the line $x^+=1/\lambda$. In particular, if μ obeys

$$\mu<\hat{\mu}(\lambda,\kappa,m)\ , \quad (3.25)$$

with

$$\hat{\mu}(\lambda,\kappa\sim16,m)\cong-\frac{e(\kappa-16)}{1024}m\lambda\ , \quad (3.26)$$

then, for black holes with $m\gg(\kappa/4)\lambda$, there will be two apparent horizons in the region $x^-<x_0^-$; one at $x_1^-\cong-m/\lambda^2-\kappa/4\lambda$ and the other at some x_2^- near $-\kappa/4\lambda$.[1] The lines of constant ϕ will be timelike for $x^-<x_1^-$, spacelike for $x_1^-<x^-<x_2^-$, and again timelike for $x^->x_2^-$. In particular, this means that the boundary curve $\phi=\phi_{cr}$ will start being timelike and therefore boundary conditions will be necessary in order to determine the evolution in the region in causal contact with the timelike boundary.

In the above discussions we have ignored terms $O(\varepsilon^2)$, and one may be concerned about their relevance. Fortunately, the solution can be exactly found near the infalling line. Following Ref. [11], we consider the equations of motion along a lightlike line infinitesimally above the matter trajectory, $x^+=1/\lambda$. On this line they are ordinary differential equations, in the variable x^-, for the quantities ∂_+X and ∂_+Y. If X_0 and Y_0 denote the linear dilaton vacuum solution, we have

$$\partial_-(\partial_+X)=Ae^{Y_0}\ , \quad (3.27)$$

$$\partial_-(\partial_+Y)=Be^{X_0}+Ce^{Y_0}\ . \quad (3.28)$$

By integrating over x^- one finds

$$\partial_+X=\mu e^{(4\lambda/\kappa)x^-}\left[\frac{\kappa}{4\lambda}-x^-\right], \quad (3.29)$$

$$\partial_+Y=\frac{4\lambda^2}{\kappa}\left[x^-+\frac{m}{\lambda^2}\right]+\lambda+\frac{4\kappa}{\kappa-16}\mu e^{(4\lambda/\kappa)x^-}\left[\frac{\kappa}{4\lambda}-x^-\right]. \quad (3.30)$$

Hence

$$\partial_+\Omega=-\frac{\lambda^2}{\sqrt{\kappa}}\left[x^-+\frac{m}{\lambda^2}\right]-\frac{\sqrt{\kappa}}{4}\lambda-\frac{\sqrt{\kappa}}{4}\frac{3\kappa-16}{\kappa-16}\mu e^{(4\lambda/\kappa)x^-}\left[\frac{\kappa}{4\lambda}-x^-\right]. \quad (3.31)$$

For $\kappa\sim16$ Eq. (3.31) reduces to Eq. (3.24) *cum* $x^+=1/\lambda$. From Eq. (3.31) we can now see that in the exact solution there are two apparent horizons if and only if μ satisfies Eq. (3.25), where the generalization to arbitrary κ of Eq. (3.26) is given by

$$\hat{\mu}(\lambda,\kappa,m)=-\frac{8e(\kappa-16)}{\kappa^2(3\kappa-16)}m\lambda\ . \quad (3.32)$$

IV. HAWKING RADIATION

Thus we see that nonperturbative corrections can easily modify the causal character of the boundary line and hence the space-time topology. It is reasonable to expect that, with suitable boundary conditions, the boundary curve will stay timelike, asymptotically approaching more null line $x^-=-v$, with $0<v<-x_0^-$. The geometry is depicted in Fig. 4, which resembles the subcritical case discussed in Sec. II (see Fig. 3). Let us assume that the system finally decays into the vacuum. At $x^+\gg1/\lambda$ the solution will take the form

$$\chi=\Omega=-\lambda^2x^+(x^-+v)-\ln[-\lambda^2x^+(x^-+v)]\ , \quad (4.1)$$

or

$$ds^2=-d\tau^2+d\sigma^2\ ,\quad \phi=-\lambda\sigma\ , \quad (4.2)$$

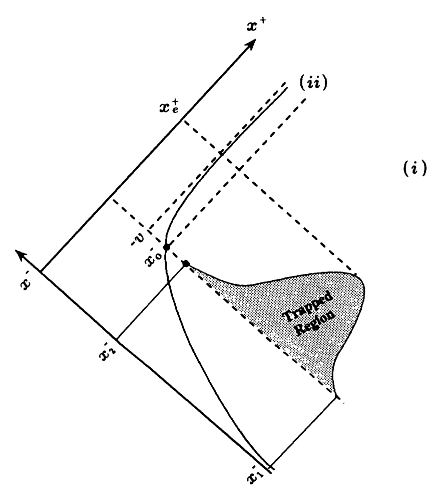

FIG. 4. Qualitative picture of black hole formation and evaporation in the model of Sec. III.

[1]Other studies of models with multiple apparent horizons describing Reissner-Nordstrom-type geometries can be found in Refs. [17,19].

where

$$e^{\lambda\sigma^+}=\lambda x^+\ ,\quad e^{-\lambda\sigma^-}=-\lambda(x^-+v)\ ,\quad \sigma^\pm=\tau\pm\sigma\ . \tag{4.3}$$

The Hawking radiation can be computed in the standard way [1] (for a derivation in the context of dilaton gravity, see Ref. [16]). It is useful to introduce Minkowski coordinates for the region $x^+<1/\lambda$:

$$e^{\lambda y^+}=\lambda x^+\ ,\quad e^{-\lambda y^-}=-\lambda x^-\ . \tag{4.4}$$

The mode expansions for the right moving field are

$$\begin{aligned} f_- &= \int_0^\infty d\omega[a_\omega u_\omega + a_\omega^\dagger u_\omega^*]\ \ (\text{in})\ . \\ &= \int_0^\infty d\omega[b_\omega v_\omega + b_\omega^\dagger v_\omega^*]\ \ (\text{out})\ , \end{aligned} \tag{4.5}$$

where

$$\begin{aligned} u_\omega &= \frac{1}{\sqrt{2\omega}}e^{-i\omega y^-}\quad (\text{in})\ , \\ v_\omega &= \frac{1}{\sqrt{2\omega}}e^{-i\omega\sigma^-}\quad (\text{out})\ . \end{aligned} \tag{4.6}$$

The in and out vacuum are defined by

$$a_\omega|0\rangle_{\text{in}}=0\ ,\quad b_\omega|0\rangle_{\text{out}}=0\ . \tag{4.7}$$

The calculation of the Bogoliubov coefficients is analogous to Ref. [16], so we will not repeat it here. For the number operator for out modes, $N_\omega^{\text{out}}=b_\omega^\dagger b_\omega$, one has

$$\text{in}\langle 0|N_\omega^{\text{out}}|0\rangle_{\text{in}}=\int_0^\infty d\omega'|\beta_{\omega\omega'}|^2\ , \tag{4.8}$$

with

$$\begin{aligned} \beta_{\omega\omega'} &= \frac{1}{2\pi\lambda}\left[\frac{\omega'}{\omega-\epsilon}\right]^{1/2}(\lambda v)^{i\omega/\lambda}B(u_1,u_2)\ , \\ u_1 &= -\frac{i}{\lambda}(\omega'+\omega)+\epsilon\ ,\quad u_2=1+\frac{i\omega}{\lambda}\ . \end{aligned} \tag{4.9}$$

At late times this leads to a thermal distribution with temperature $T_H=\lambda/2\pi$ [16], as is characteristic of two-dimensional models [27].

The expectation value of the energy momentum tensor, ${}_{\text{in}}\langle 0|T^f_{\mu\nu}|0\rangle_{\text{in}}$, asymptotically in the out region $\mathcal{I}_+$, is computed in the standard way by normal ordering with respect to b_ω, $b_\omega^\dagger$, i.e., one requires ${}_{\text{out}}\langle 0|T^f_{\mu\nu}|0\rangle_{\text{out}}=0$. The result is

$${}_{\text{in}}\langle 0|T^{(i)}_{--}|0\rangle_{\text{in}}=\frac{\kappa}{4}\left[\frac{1}{(x^-+v)^2}-\frac{1}{x^{-2}}\right]\ . \tag{4.10}$$

In region (ii) the precise form will depend on the boundary conditions.

Note that $T^{(i)}_{--}$ vanishes for $x^-\ll -v$,

$$T^{(i)}_{--}\sim -\frac{\kappa}{2}\frac{v}{x^{-3}}\ ,\quad x^-\ll -v\ .$$

In particular, if $m\gg\kappa\lambda$, T_{--} will be negligible at the fake event horizon at $x^-\cong -m/\lambda^2$. In fact, it is clear that most of the energy will be radiated far beyond $x^-=-m/\lambda^2$, in contrast with the usual picture of Hawking radiation. At $x^-=-m/\lambda^2$, the Bondi mass will be of the same order of the total ADM energy carried by the shock wave. Indeed, the total energy radiated out in region (i) is

$$\begin{aligned} E^{(i)}_{\text{out}} &= -\lambda\int_{-\infty}^{x_0^-}dx^-(x^-+v)T^{(i)}_{--}\ , \\ &= \lambda^2 v-\frac{\kappa\lambda}{4}\ln\left[1-\frac{4\lambda v}{\kappa}\right]\ , \end{aligned} \tag{4.11}$$

which is a Planck-order energy. The Hawking temperature is the same but the radiation comes out at later times. The boundary conditions will dictate how much of the total energy will originate from pure reflection off the boundary, and how much of it will be carried out as Hawking radiation.

In the usual semiclassical picture one assumes that the final state has the form

$$\chi=\Omega=-\lambda^2x^+\left[x^-+\frac{p}{\lambda^2}\right]-\ln\left[-\lambda^2x^+\left[x^-+\frac{p}{\lambda^2}\right]\right]\ , \tag{4.12}$$

with $p\cong m$. Quantum fluctuations of the end-point position can only correct p by a Planck-order energy, and therefore Eq. (4.12) and the consequent outgoing Hawking radiation should not receive important corrections for macroscopic black holes. However, we have just seen that if the actual boundary of the space time is timelike, there is no way the final state can have the form (4.12). It will be given by Eq. (4.1), which is different from (4.12) in an important way, as far as the problem of information loss is concerned.

Given the geometry of Fig. 4, an observer who never crosses the null line $x^-=-m/\lambda^2$ will undergo acceleration all the time, approaching the speed of light as $t\to\infty$. As a result, he will be immersed in a bath of thermal radiation, detecting the same outgoing radiation that one would calculate if the vacuum were given by Eq. (4.12). For $x^-\ll -m/\lambda^2$ a distant observer will detect the usual Hawking radiation with respect to the false vacuum (4.12). The vacuum (4.1) has a well-understood physical meaning, i.e., the absence of particles according to all inertial observers in the asymptotic region.

V. NUMERICAL ANALYSIS FOR SPECIFIC MODELS OF BLACK HOLE EVAPORATION

Let us consider a scenario in which the linear dilaton vacuum receives a Planck-order nonperturbative correction, $\mu_{ldv}=O(\lambda^2)$. For definiteness let us take [see Eqs. (3.25) and (3.32)]

$$\mu=\hat\mu+\mu_{ldv}=-\frac{8e(\kappa-16)}{\kappa^2(3\kappa-16)}m\lambda+\mu_{ldv}\ , \tag{5.1}$$

$$\mu_{ldv}=\hat\mu\left[\lambda,\kappa,m=\frac{\kappa}{4}\lambda\right]\ . \tag{5.2}$$

The qualitative time evolution of the geometry is independent of m, as long as m is much greater than the Planck mass. For $m\sim(\kappa/4)\lambda$ some anomalous behavior occurs (in virtue of a collapsing of the apparent horizons), but the present semiclassical approximation is not supposed to apply for black holes of Planckian masses. So let us restrain our attention on macroscopic black holes. A typical Kruskal diagram is exhibited in Figs. 5 and 6. These plots have been made with $\lambda=1$, $\kappa\cong 16$, and $m=20$. Many other cases of $\kappa>16$ and m have also been investigated, in essence obtaining the same picture.

The geometry agrees with the standard semiclassical configuration (see Fig. 2) in weak-coupling regions which are not in causal contact with strong-coupling regions. The inner apparent horizon starts on $x^+=l/\lambda$ at some x^- near x_0^- (Fig. 6), and it joins the outer apparent horizon at the end point of the trapped region, $x^+=x_e^+$ (see Appendix). In addition there is another apparent horizon with $\partial_-\Omega=0$, but it entirely resides in a region where the perturbative method to solve the differential equations is not very reliable. It is unclear whether this apparent horizon will subsist in the exact solution. In the case of Fig. 5, it approaches asymptotically the null line $x^-=-m/\lambda^2$, but the approximation breaks down much earlier, as indicated in Fig. 6. The contours of constant Ω have

$$\frac{dx^+}{dx^-}=-\frac{\partial_-\Omega}{\partial_+\Omega}\ ,$$

so they cross the apparent horizons with $\partial_-\Omega=0$ and $\partial_+\Omega=0$ with derivatives equal to zero and infinity, respectively.

There is a naked singularity at the timelike curve $\Omega=\Omega_{\rm cr}$, so boundary conditions are needed for the continuation to region (ii). This time the simplest choice Eq. (2.8) cannot be implemented, as can be easily verified. Conceivably the boundary conditions are also corrected by nonperturbative terms. However, from Eq. (2.7) it seems clear that boundary conditions which do not obey Eq. (2.8) will necessarily lead to naked singularities, presumably leading to instabilities. A black hole could evolve into an object carrying an arbitrary amount of negative energy and then continue to radiate *in secula seculorum*. This feature could be an artifact of the particular model we have contemplated, or simply an artifact of the semiclassical approximation.

Other possible extensions of the solution are suggested in Figs. 7(a) and 7(b). In order to avoid a remnant scenario, the solution must approach the linear dilaton vacuum for late times x^+. The necessary condition is that, for $x^-\leq x_0^-$ and $x^+\gg 1/\lambda$, Ω takes the form (4.1). Unfortunately, the present approximation for solving the differential equations (3.7), (3.8) breaks down as $\varepsilon=O(1)$ (Fig. 6). At $x^-=x_0^-$ this corresponds to

$$x^+\sim\frac{m}{\lambda(m-(k/4)\lambda)}\ .$$

So the exact solution is necessary to decide whether the matching with the linear dilaton vacuum on $x^-=x_0^-$ and $x^+\gg 1/\lambda$ is feasible for this specific model.

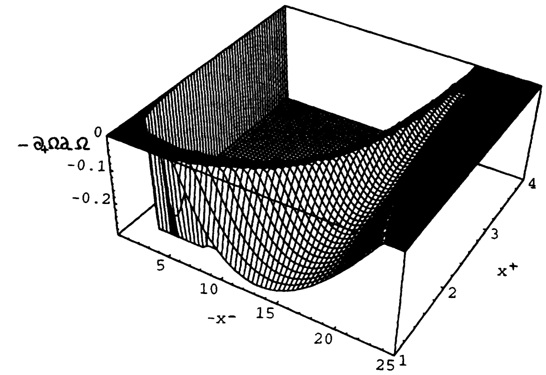

FIG. 6. Plot of $-\partial_+\Omega\partial_-\Omega$ as a function of x^+, x^- in the geometry of Fig. 5. Negative values represent the trapped region, whose boundary is the apparent horizon. Positive values have been truncated.

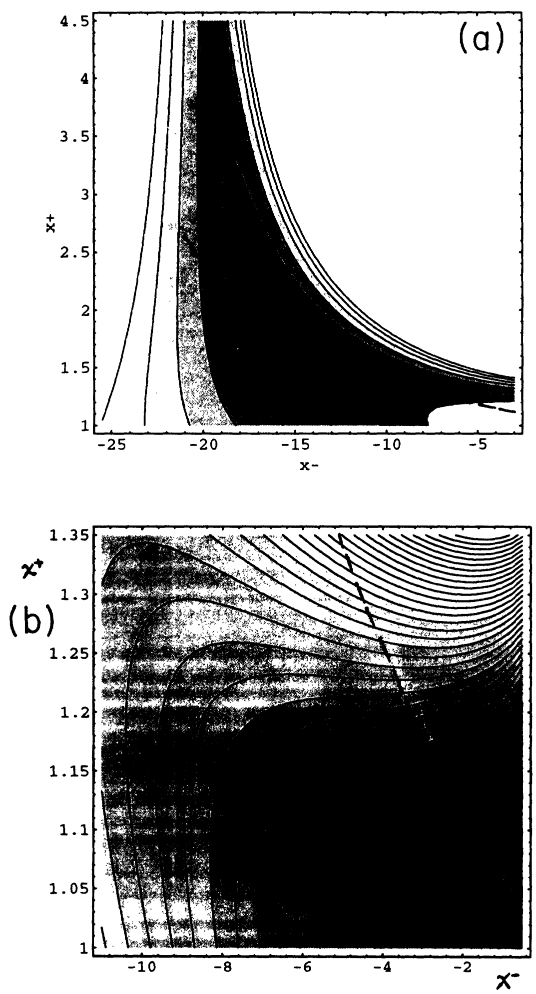

FIG. 5. Geometry corresponding to the model of Sec. V, illustrated by numerical plots of contours of constant ϕ. The dashed line indicates the region where the present approximation begins to break down. (a) and (b) show different regions and scales of the same configuration. The thick line in (b) corresponds to $\phi=\phi_{\rm cr}$.

Without a cognition of the asymptotic behavior of the solution in $\mathscr{I}_+$ and in region (ii) it is not possible to determine the outgoing spectrum of Hawking radiation. For physical reasons, it is likely that the boundary curve will stay timelike, and it is conceivable that the system will finally decay into the vacuum. Then the discussion of Sec. IV will apply and, in particular, the outgoing energy-momentum tensor will be given by Eq. (4.10). Meanwhile, it is interesting to look at local quantities which in certain limits are related to the Bondi mass of the black hole, for example, the value of $e^{-2\phi}$ at the outer apparent horizon. In the case of Fig. 5, $m=20$, $\lambda=1$, $\kappa\sim 16$, one finds by numerical computation that

$$e^{-2\phi}|_{x^+=x_e^+}=16.6\cong O\left[\frac{m}{\lambda}\right]. \tag{5.3}$$

This is unlike the $\mu=0$ RST case, where $e^{-2\phi}$ at the end point is of Planck order. The apparent horizon deviates from the $\mu=0$ apparent horizon at earlier times than expected. We have verified that this feature is independent of any particular choice of the parameters, i.e., for macroscopic black holes $e^{-2\phi}$ at x_e^+ seems to be, roughly, of the same order as m/λ, which suggests that most of the energy will be radiated far beyond $x^-=-m/\lambda^2$. For example, for $m=40$ and $m=80$ one finds, respectively, $e^{-2\phi}|_{x^+=x_e^+}=21.5$ and $e^{-2\phi}|_{x^+=x_e^+}=24.8$. Unfortunately, there are numerical problems to study the case of larger masses. While the nonperturbative term we added to the action is insignificant at the end point, the fields Ω and χ, being integrals of this, receive nonnegligible corrections near the end point. Indeed, to the leading order in perturbation theory we are making, Ω and χ contain terms of the form $\mu\varepsilon/(x^-+m)$. For a very massive black hole, ε is exponentially small at the end point of the trapped region, but x^- is exponentially close to $-m$, giving rise to a contribution of order unity. This explains why there seem to be some changes in local quantities at the end point of the trapped region. However, one must be careful in extracting conclusions from this, since the present leading-order approximation could be simply breaking down before getting to the end point. Certainly, it would be interesting to have the exact solution to the differential equations (3.7) and (3.8), but the application of the present model to illustrate a no-veil scenario is only limited to early times. The full theory of quantum dilaton gravity is presently unknown. This would permit a systematic derivation of nonperturbative corrections, and thereby a better control of the approximations in a phenomenological model containing nonperturbative effects.

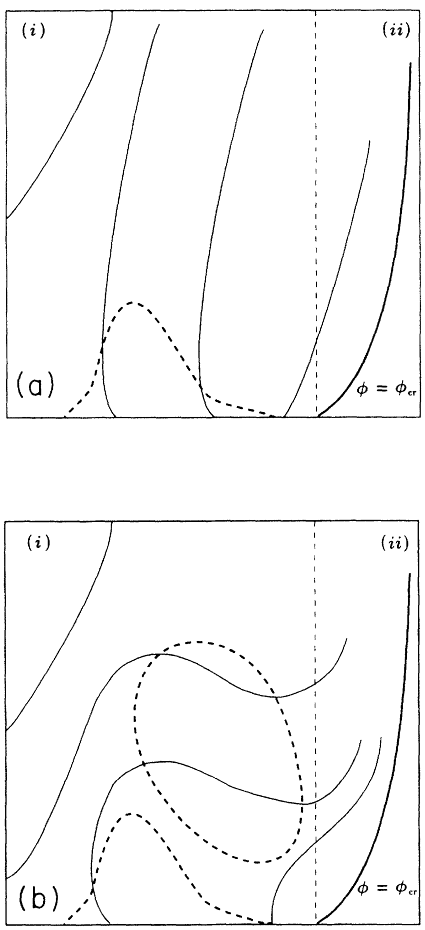

FIG. 7. Possible extensions of the geometry of Fig. 5 into the region where the solution to the differential equations (3.7) and (3.8) is unknown. (a) The apparent horizon with $\partial_-\Omega=0$ is absent; (b) the apparent horizon with $\partial_-\Omega=0$ is present, but it is closed, confined to a finite region in space-time.

VI. NO COSMOLOGICAL VEIL CONJECTURE

In Secs. III and V we have seen simple models where additional quantum corrections turn the spacelike boundary into a timelike boundary, altering the topology of the standard semiclassical picture of black hole evaporation. In these models there is no longer a clear problem of information loss, since all information might return by simply reflecting back on the boundary curve.

It has long been speculated that quantum effects might prevent singularities from occurring or might smooth them out in some way. If this is the case, it is plausible that the spacelike boundary will be absent and thus no global horizon will appear in a full quantum treatment, since otherwise the space time would be geodesically incomplete. A similar phenomenon should occur in other cases of topology change.

As far as the resolution of the information problem is concerned, the topology does not need to be trivial. For example, there could be a conical singularity at the end point, as indicated in Fig. 8. A large wormhole would carry all the information back in region (ii).[2]

[2]Geometries of this type, in connection with the problem of information loss, were investigated in Ref. [5]. However, the interpretation given in Ref. [5] is quite different from the more straightforward interpretation considered in this paper.

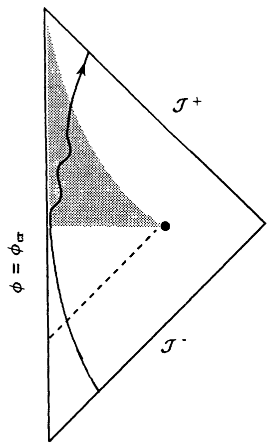

FIG. 8. An alternative topology instead of Fig. 1(b) which would lead to similar results.

The no cosmic veil conjecture may be formulated in a simple way:

Quantum effects preclude the formation of global event horizons.

That a global event horizon cannot be a strict "point of no return" in a quantum theory is obvious, since in quantum mechanics it is not possible to localize, e.g., the end point or any branching point with an infinite accuracy. However, for large black holes, the fluctuations in the position of the event horizon can be neglected compared to the Schwarzchild radius. The above conjecture affirms that there are no global event horizons, not even in an approximative sense.

Let us consider a black hole-type configuration with mass much larger than the Planck mass. What will an outside observer see? Freely falling matter will pass through the outer apparent horizon, then enter into a strong coupling region, experiencing Planckian curvatures, and eventually will reflect back at zero radial coordinate. An outside, timelike observer, far away from the black hole, will probably measure some shock wave coming out at time $x^-=-m/\lambda^2$, originating from the end point of the trapped region (see Ref. [28]). Finally, he will be in causal contact with the timelike boundary, recovering all the energy and the quantum mechanical information, including global quantum numbers (unless boundary interactions violate the corresponding global symmetry).

VII. CRITIQUE

Without pretense of a deep inquiry at this primitive stage, it may be worth mentioning a number of points which evoke skepticism. To begin with, the examples investigated in this paper, though introduced only for illustrative purposes, are rather *ad hoc* and represent an oversimplified sample of nonperturbative corrections. The mere inclusion of other terms in the potential (3.4) could modify the picture, maybe in a favorable way, but maybe unfavorably. What is more significant is the issue of the boundary conditions. This is important in order to define a setting for the construction of an S matrix. For stability reasons, one would like to demand Eq. (2.8) on the boundary so as to ensure finite curvature everywhere. It is necessary to have a timelike line starting at $\phi=\phi_{cr}$ with $\partial_+\Omega=0$. In the numerical study there was no way to achieve this, irrespective of the choice of parameters, which jeopardizes the implementation of the boundary conditions. It would be interesting to show that, e.g., by adjusting different parameters of the potential (3.4), one can have the structure of Fig. 4 and a timelike line starting at $\phi=\phi_{cr}$ with $\partial_+\Omega=0$ (which shall be the boundary curve after implementation of boundary conditions). A last recourse is invoking new degrees of freedom for the space-time boundary. A related point is that, even in the specific examples provided in Sec. V, there is not enough evidence to believe that the geometry will eventually decay into the vacuum. It might approach some static solution, producing a remnant scenario.

Leaving aside the two-dimensional example and its problems, the proposal for the resolution of the information problem maintains a conservative viewpoint in the sense that it does not lead to violation of the standard laws of quantum mechanics and thermodynamics, and in weak-coupling regions, which are not in the causal future of strong-coupling regions, it locally agrees with the usual semiclassical picture. It is somewhat radical in the sense that it resolves the information problem by removing from the stage the very origin of the paradox—the black holes. Nevertheless, it is not at all clear why there should always be an inner apparent horizon (or an odd number of inner apparent horizons), insensitive to distinct cases of Cauchy data, which would permit the space-time boundary to align to a timelike direction.

Regrettably, the alternatives, called (1) and (2) in the Introduction, seem to be excluded for insurmountable reasons. Lacking enough justification to support the no-veil conjecture, this remains a theoretical caprice. Clearly, there is much work to be done.

Note added: In a recent study severe constraints to the no-veil scenario have been found [28]. In particular, there must be a shock wave carrying Planckian curvature at the end point of the trapped region and regions with negative energy density.

ACKNOWLEDGMENTS

The author wishes to thank J. Polchinski, L. Susskind, and L. Thorlacius for valuable discussions. This work was supported in part by NSF grant PHY 9009850 and R. A. Welch Foundation.

APPENDIX: APPARENT HORIZONS IN TWO DIMENSIONS

The apparent horizon plays an important role in the mechanisms described in the main text, and it is also a very useful and physically meaningful object in the standard picture of black hole formation and evaporation. Thus it is worthwhile to refresh the connection with the standard four-dimensional definition (see, e.g., Ref. [29]).

Let C be a three-dimensional manifold with boundary S. Let ξ_μ, $\mu=0,1,2,3$, be the vector field of tangents to a congruence of outgoing null geodesics orthogonal to S. C is a *trapped region* if the expansion $\theta=\nabla_\mu\xi^\mu$ is everywhere nonpositive on S, $\theta \le 0$. The *apparent horizon* $\mathcal{A}$ is the boundary of the *total trapped region,* the latter defined as the closure of the union of all trapped regions. A corollary of this definition is that $\theta=0$ on $\mathcal{A}$.

Now let us contemplate metrics of the form

$$ds^2=g_{ij}(x^0,x^1)dx^i dx^j+\exp[-2\phi(x^0,x^1)]d\Omega^2 \ , \tag{A1}$$

where $i,j=0$, 1. In this spherically symmetric space time we have $\xi_\mu=\{\xi_0,\xi_1,0,0\}$, and the geodesic equation reduces to

$$\xi^i\nabla_i\xi^j=0 \ , \tag{A2}$$

i.e., the two-dimensional geodesic equation. Since in this dimensionally reduced configuration there is only one family of outgoing null geodesics, a trapped region is the total trapped region, and the condition determining the apparent horizon simply becomes

$$\theta=0 \ . \tag{A3}$$

From Eq. (A1) one easily obtains

$$\theta=\theta^{(2)}-2\xi^j\partial_j\phi \ . \tag{A4}$$

where

$$\theta^{(2)}\equiv\partial_i\xi^i+\Gamma^i_{ij}\xi^j \ . \tag{A5}$$

Let us denote $B_{ik}=\nabla_i\xi_k$. By using the geodesic equation $\xi^i B_{ik}=0$, and the fact that ξ is null, $\xi^i\xi_i=0$, one derives the following relations:

$$\xi^1 B_{11}=-\xi^2 B_{21} \ , \quad \xi^1 B_{21}=-\xi^2 B_{22} \ , \quad B_{12}=B_{21} \ , \tag{A6}$$

thereby we obtain

$$\theta^{(2)}=g^{ij}B_{ij}=B_{11}\left[g^{11}-2\frac{\xi^1}{\xi^2}g^{12}+\left[\frac{\xi^1}{\xi^2}\right]^2 g^{22}\right] =0 \ , \tag{A7}$$

where we have used $\xi^1\xi_1=-\xi^2\xi_2$. Thus we see that the two-dimensional expansion parameter is identically zero. This means that an intrinsically two-dimensional apparent horizon cannot be defined. Now, by using Eqs. (A3), (A4), and (A7) we find that the condition defining the apparent horizon becomes

$$\xi^i\partial_i\phi=0 \ . \tag{A8}$$

Since ξ is null, Eq. (A8) implies $\xi_i=f(x)\partial_i\phi$, where $f(x)$ is a function. Therefore the condition (A3) gives

$$g^{ij}\partial_i\phi\partial_j\phi=0 \ . \tag{A9}$$

In the conformal gauge Eq. (A9) reduces to

$$\partial_+\phi\partial_-\phi=0 \ . \tag{A10}$$

Therefore the apparent horizon $\mathcal{A}$ is the locus of $\partial_+\phi\partial_-\phi$. In terms of $\Omega(\phi)$, Eq. (A10) reads

$$\frac{1}{\Omega'^2}\partial_+\Omega\partial_-\Omega=0 \ , \tag{A11}$$

that is, provided $\Omega'\neq 0$, the points satisfying $\partial_+\Omega=0$ or $\partial_-\Omega=0$ define the position of the apparent horizon. In the critical line one may have $\partial_+\Omega=\partial_-\Omega=0$, but $\partial_+\phi\partial_-\phi\neq 0$, as occurs in the subcritical case of Sec. II when the boundary conditions (2.8) are applied.

[1] S. W. Hawking, Commun. Math. Phys. **43**, 199 (1975); Phys. Rev. D **14**, 2460 (1976).

[2] D. N. Page, Phys. Rev. Lett. **44**, 301 (1980); T. Banks, M. Peskin, and L. Susskind, Nucl. Phys. **B244**, 125 (1984).

[3] G. 't Hooft, Nucl. Phys. **B335**, 138 (1990).

[4] L. Susskind, L. Thorlacius, and J. Uglum, Phys. Rev. D **48**, 3743 (1993).

[5] C. R. Stephens, G. 't Hooft, and B. F. Whiting, University of Utrecht Report Nos. THU-93/20 and UF-RAP-93-11, 1993 (unpublished).

[6] J. G. Russo, L. Susskind, and L. Thorlacius, Phys. Rev. D **46**, 3444 (1992).

[7] J. G. Russo, L. Susskind, and L. Thorlacius, Phys. Rev. D **47**, 533 (1993).

[8] C. G. Callan, S. B. Giddings, J. A. Harvey, and A. Strominger, Phys. Rev. D **45**, R1005 (1992).

[9] J. G. Russo and A. A. Tseytlin, Nucl. Phys. **B382**, 259 (1992).

[10] T. Banks, A. Dabholkar, M. R. Douglas, and M. O'Loughlin, Phys. Rev. D **45**, 3607 (1992).

[11] J. G. Russo, L. Susskind, and L. Thorlacius, Phys. Lett B **292**, 13 (1992).

[12] B. Birnir, S. B. Giddings, J. A. Harvey, and A. Strominger, Phys. Rev. D **46**, 638 (92); S. W. Hawking, Phys. Rev. Lett. **69**, 406 (92); L. Susskind and L. Thorlacius, Nucl. Phys. **B382**, 123 (1992).

[13] A. Strominger, Phys. Rev. D **46**, 4396 (1992).

[14] A. Bilal and C. G. Callan, Nucl. Phys. **B394**, 73 (1993); S. P. de Alwis, Phys. Lett. B **289**, 278 (1992); *ibid.* **300**, 330 (1993).

[15] S. B. Giddings and A. Strominger, Phys. Rev. D **47**, 2454 (1993).

[16] S. B. Giddings and W. Nelson, Phys. Rev. D **46**, 2486 (1992).

[17] T. Banks and M. O'Loughlin, Phys. Rev. D **48**, 698 (1993).

[18] D. Lowe, Phys. Rev. D **47**, 2446 (1993); A. Strominger and S. Trivedi, *ibid.* **48**, 5778 (1993).

[19] D. Lowe and M. O'Loughlin, Phys. Rev. D **48**, 3735 (1993).

[20] S. W. Hawking and J. M. Stewart, University of Cambridge Report No. PRINT-92-0362, 1992 (unpublished).

[21] Y. Park and A. Strominger, Phys. Rev. D **47**, 1569 (1993); A. Bilal, *ibid.* **48**, 1665 (1993).

[22] T. Banks, M. O'Loughlin, and A. Strominger, Phys. Rev. D **47**, 4476 (1993).

[23] E. Verlinde and H. Verlinde, Princeton Report No. PUPT-1380, IASSNS-HEP-93/8, 1993 (unpublished); K. Schoutens, E. Verlinde, and H. Verlinde, Phys. Rev. D **48**, 2670 (1993).

[24] S. W. Hawking and J. D. Hayward, University of Cambridge and CalTech Report Nos. DAMTP-R93-12 and CALT-68-1861 (unpublished).

[25] D. N. Page, University of Alberta Report No. Alberta-Thy-23-93, 1993 (unpublished).
[26] F. David, Mod. Phys. Lett. **A3**, 1651 (1988); J. Distler and H. Kawai, Nucl. Phys. **B321**, 509 (1989).
[27] E. Witten, Phys. Rev. D **44**, 314 (1991).
[28] J. G. Russo, "On Black Hole Singularities in Quantum Gravity," University of Texas Report No. UTTG-32-93, 1993 (unpublished).
[29] R. M. Wald, *General Relativity* (University of Chicago, Chicago, 1984).

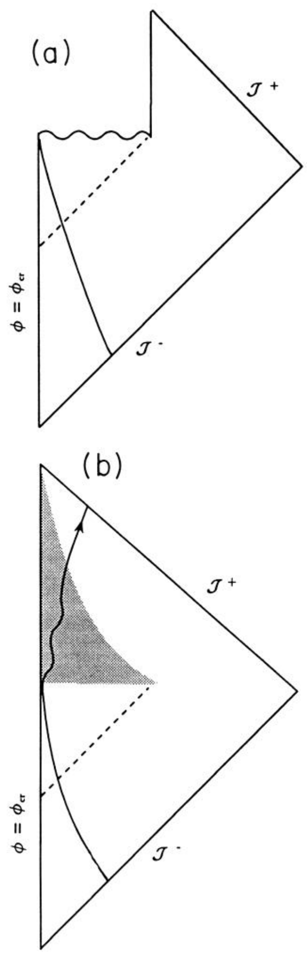

FIG. 1. (a) Penrose diagram corresponding to the standard semiclassical picture of black hole evaporation. (b) Penrose diagram of another geometry which differs from Fig. 2(a) only in the strong curvature region. In the scenario there is no spacelike boundary.

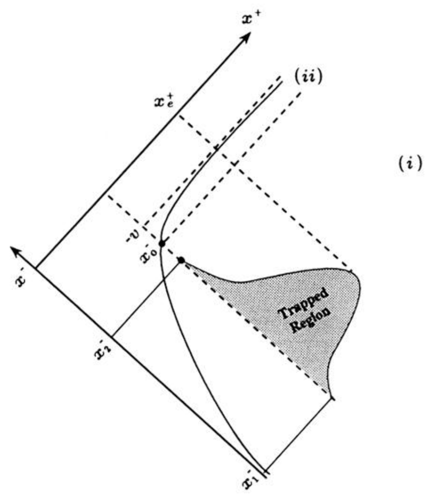

FIG. 4. Qualitative picture of black hole formation and evaporation in the model of Sec. III.

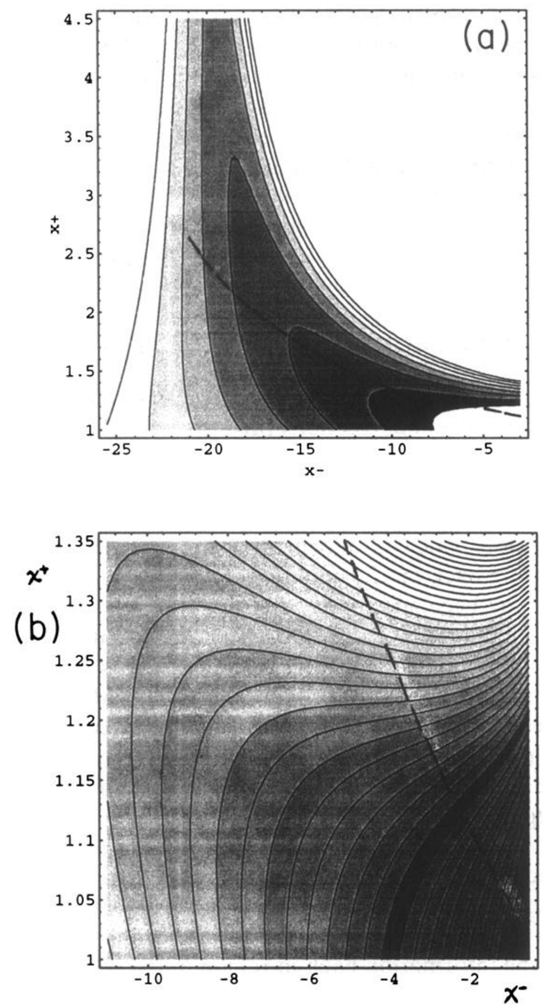

FIG. 5. Geometry corresponding to the model of Sec. V, illustrated by numerical plots of contours of constant ϕ. The dashed line indicates the region where the present approximation begins to break down. (a) and (b) show different regions and scales of the same configuration. The thick line in (b) corresponds to $\phi=\phi_{\rm cr}$.

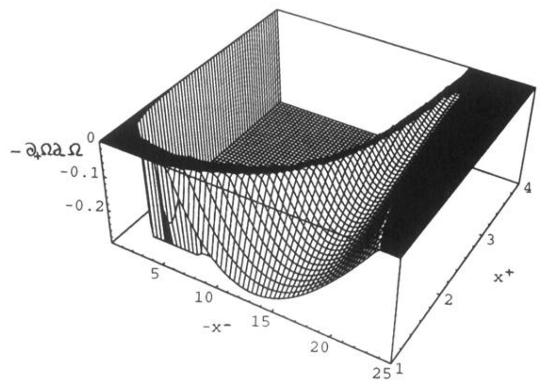

FIG. 6. Plot of $-\partial_+\Omega\partial_-\Omega$ as a function of x^+, x^- in the geometry of Fig. 5. Negative values represent the trapped region, whose boundary is the apparent horizon. Positive values have been truncated.

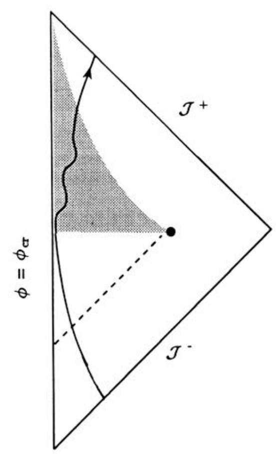

FIG. 8. An alternative topology instead of Fig. 1(b) which would lead to similar results.